Wireless Pers Commun (2015) 83:1713–1730
DOI 10.1007/s11277-015-2472-5

Design and Performance Study of Sierpinski Fractal Based Patch Antennas for Multiband and Miniaturization Characteristics

P. Satish Rama Chowdary · A. Mallikarjuna Prasad · P. Mallikarjuna Rao · Jaume Anguera

Published online: 6 March 2015

Abstract Modern wireless communication systems demand for compact and miniaturised antennas which are capable of operating at multiple frequency bands. Cutting fractals on traditional geometry and using them as antennas for such applications have a wide scope of research. In this work, Sierpinski geometry based patch antenna is considered for multiband operation and miniaturisation of the radiating element. The characteristics of the fractal based antennas are investigated as a function of fractal iteration. The fabricated prototypes are used to validate the simulated results.

Keywords Fractal · Patch antenna · Sierpinski · Bowtie · Multiband · Miniaturisation

1 Introduction

The world has witnessed several fascinating revolutions in the field of telecommunications during the transition from twentieth century to twenty-first century. Among those wireless

P. S. R. Chowdary (✉)
Department of ECE, Raghu Institute of Technology, Visakhapatnam, India
e-mail: psrsatissh@gmail.com; psr_satish@yahoo.com

A. M. Prasad
Department of ECE, UCE (A), JNTUK, Kakinada, India
e-mail: a_malli65@yahoo.com

P. M. Rao
Department of ECE, AUCE(A), Andhra University, Visakhapatnam, India
e-mail: pmraoauece@yahoo.com

J. Anguera
Department of Electronics and Telecommunications, University Ramon Llull, Barcelona, Spain
e-mail: jaumean@salleurl.edu

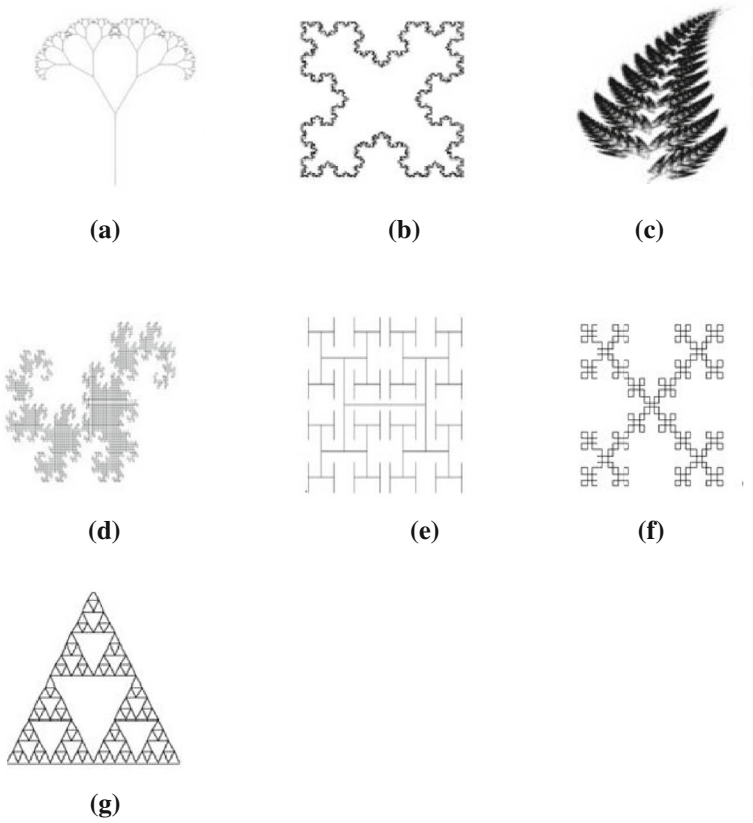

Fig. 1 Geometrical shapes of some fractal geometry. **a** Tree Fractal, **b** Cesàro fractal, **c** Barnsley's fern. **d** Dragon curve, **e** H-fractal, **f** Sierpinski square, **g** Sierpinski triangle

revolution has provided mobile communication, Global Positioning System, Wireless LAN, WiMax, WiFi, LTE and many other services [1]. These wireless communication techniques support fast data transmission [2–4] rate and novel modulation techniques. In addition to these, the wireless revolution has made the electronic system small and compact. Antenna in such a wireless system is responsible for radiating and receiving electromagnetic waves for communication. Besides these in the modern wireless systems the antenna has to adapt the following functionalities.

- Needs to handle large amounts of data in short period of time, which means it needs to possess broadband characteristics.
- An antenna designed for a particular operating frequency exhibits good characteristics for that frequency and may not have fully functional operation at other frequencies. Most of the telecommunication systems operate at separate frequencies to avoid the interference. Hence one may have accommodated dedicated antennas for every operating frequency. To avoid this one antenna capable of operating at all the required frequencies is good practice. For this the antenna need to be multifrequency or frequency independent.

- Owing to the modern communication devices like mobile radio and handheld communication systems, the antenna has to be conformal with the compactness of the system and environment. This is achieved with miniaturisation of the antenna.
- Most of the Miniaturised antennas have poor radiation efficiency and directivity. One would be interested in making a small antenna a better radiator for example by using low loss dielectric and stacking patches.

In this paper multiband and miniaturisation characteristics of planar fractal based antennas are studied. The fractals are carved on microstrip patch antennas and are explored to meet the above requirements. The study and analysis is based on the simulation of the geometry and measured data on the fabricated prototypes. The study of multiband characteristics is based on the Sierpinski geometry. The Sierpinski Bowtie (SPKBT) geometry is used for studying the miniaturisation characteristics. The entire investigation on the miniaturisation is subdivided into four cases starting from a square patch in case 1 to a SPKBT of third iteration in case 4. For each geometry analysis basing on the reflection coefficient, radiation pattern, and frequency versus Directivity reports are presented.

1.1 Microstrip Patch Antennas

High frequency structure simulation (HFSS) tool based on finite element method (FEM) numerical technique is used for simulation throughout this work. All the geometries proposed in this work belong to the basic category of microstrip patch antennas (MPA). The Microstrip Antenna (MA) technology is heard for the first time during 1950s as novel feeding techniques to achieve enhanced BW, Gain and for accurate prediction of the numerically analysed results. The choice of MPA is always backed up with its advantages with respect to its structure. An MPA is low profile, low cost, conformal to the device structure, low volume. The electrical characteristics of the MPA are supportive to both dual and circular polarization. The resonant characteristics of the antenna are easily controllable with its dimensions. They are compatible and easy adaptable with every system. On the other side there are some drawbacks with this antenna type. They have a very narrow bandwidth. As a single element antenna it exhibits limited beam steering and has radiation pattern which is hardly controllable.

1.2 Fractal Geometry

The concept of combining the fractal geometry (FG) with electromagnetic is analyzed. The word antenna is often prefixed with the word latest which gives the state of research in the field. In the latest antenna research the fractal geometry plays a vital role. It is a powerful means of describing any geometrical shapes. The shapes of Coast line, leaf, clouds etc. are some complex phenomenon that are described effectively using fractals [1]. This

Fig. 2 Variation in area from **a** generation 1 and iteration 0 through **d** generation 4 and iteration 3 in Sierpinski geometry

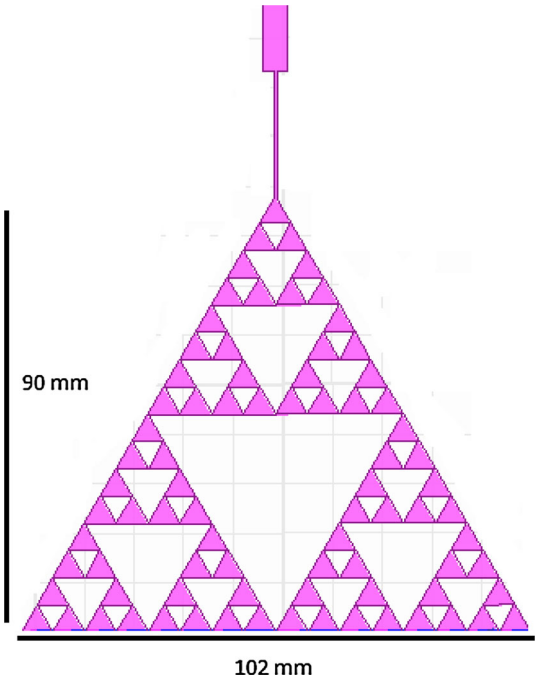

Fig. 3 Geometry of the SPK after 5th iteration

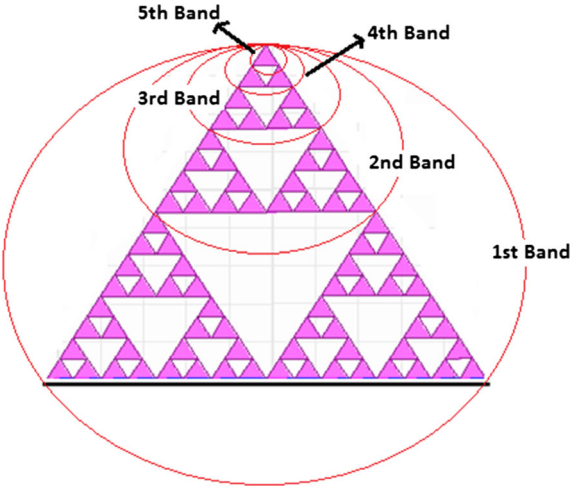

Fig. 4 Band representation of the SPK5

magnificent strategy has drawn the attention of many elites from mathematics, computer science, statistics, image and signal processing and electromagnetic group. Earlier the objects are classified using Euclidean geometry as one, two and three dimensional. The objects in the world are not described using Euclidean geometry. Here comes the application of FG. The fractals have the properties like (a) Self Similarity, (b) Fractional Dimension and (c) Fractal boundaries.

The self similarity property of the FG can be easily explained with the geometry with shape within shape. The fractional dimension property of the FG does the job of space

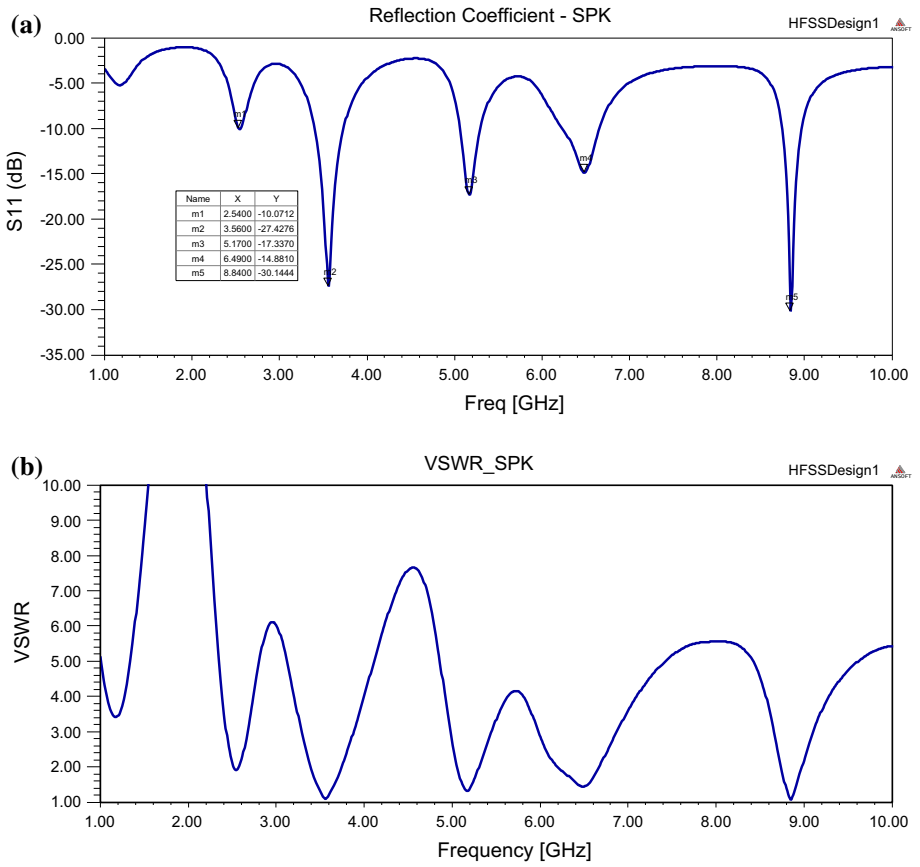

Fig. 5 **a** Simulated reflection coefficient plot of SPK5. **b** VSWR plot of SPK5

filling. The third property i.e., fractal boundaries can explain in two ways like mass fractals and boundary fractals. Mass fractals have their internal structure a fractal again. Boundary fractal has the boundaries (outer structures) of the regular shape as fractals.

Considering these excellent properties listed above the FG are applied to the antenna field. Much new geometry has been derived from Mandelbrot's "Concept of New Geometry" [5]. Some of them are very popular in serving as radiating elements. Among those, Sierpinski triangle and Sierpinski carpet are named after Sierpinski (1916), Hilbert curves named after Hilbert.D (1891), Koch curves named after Koch.V.H (1904), Julian structures named after Julia.G (1918) and Contor shapes named after Contor.G (1872) have wide applications in electromagnetic with their vital electrodynamics. Some fractal shapes are presented in the following Fig. 1.

2 Multiband Characteristics of Sierpinski

The basic geometry of the Sierpinski (SPK) is as mentioned in the Fig. 1g is considered here. An SPK has various flavors of construction. These variations are observed with respect to the point of view, rotation and scaling. The multiband behavior of the fractal

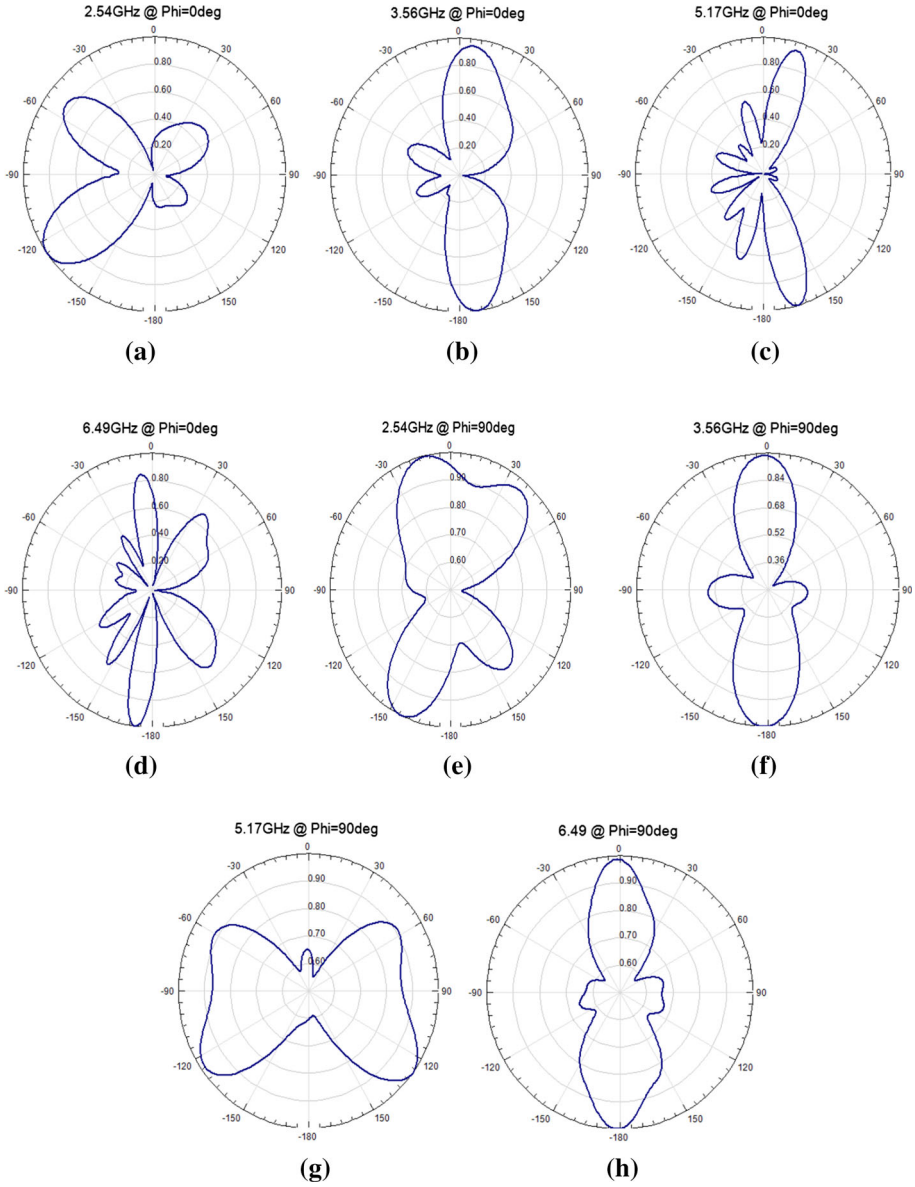

Fig. 6 Radiation patterns of the antenna at .54, 3.56, 5.17, 6.49 GHz resonant frequencies for Ø = 0°

shaped SPK is described by Lizzi et al. [6], Werner and Werner [7], Mushiake [8], Chowdary et al. [9], Vinoy et al. [10], Puente-Baliarda et al. [11], Anagnostou et al. [12], Na and Xiao-wei [13], and further a comparative study between the SPK monopole and dipole is also presented in it. The resultant log periodic behavior of the SPK is due to the self similarity property of it. The dimension of the FG is measured using the following formula.

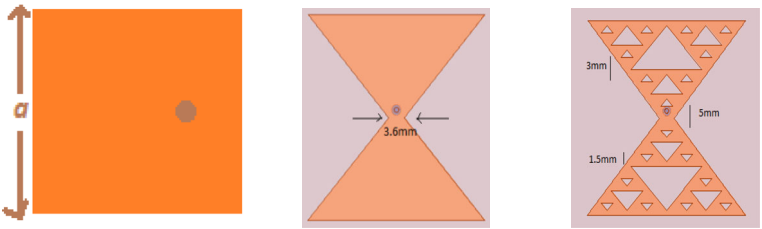

Fig. 7 Transition of geometry from square to SPKBT-2. **a** Square patch, **b** Bowtie, **c** SPKBT-2

$$\mathrm{D} = \mathrm{Log\ N(number\ of\ new\ pieces)/Log\ M(Magnification:\ factor\ of\ finer\ resolution)}$$

For the SPK with respect to the Fig. 1g the dimension is calculated as

$$\mathrm{D} = \log_2(3) = 1.584 \tag{1}$$

where the scaling factor is 2 and the number new pieces formed are 3.

2.1 Effective Area Considerations in SPK

A triangle is the initiator for SPK triangle geometry. In every iteration a scaled down triangle of its previous iteration is tweaked out. For each iteration the circumference and the area varies. If a triangle of unit area is considered then after the first iteration 1/4 of the area is removed. Consequently after the second and third iteration, 3/16 and 9/64 of the area is removed respectively as shown in the Fig. 1. The generalized expression for this phenomenon is given by

$$A_N = 1/3 \sum_{i=1}^{N} (3/4)^i \tag{2}$$

where A_N refers to the area removed. From the above equation it can be inferred that after infinite iterations $A_\infty = 1$. This means that the resultant gasket has no area but has infinite circumference. The same is depicted in the Fig. 2a–d. The triangle in Fig. 1a is considered to have $A_0 = 1$ area then, the corresponding generations from (b) through (d) will have areas A_1, A_2, and A_3 given as

$$A_1 = (3/4)A_0, \tag{3a}$$

$$A_2 = (3/4)^2 A_0 \tag{3b}$$

$$A_3 = (3/4)^3 A_0 \tag{3c}$$

2.2 Formulation of Resonant Frequencies

The analytical estimation of the resonant frequencies of a Sierpinski monopole after n iterations is as mentioned below by [14].

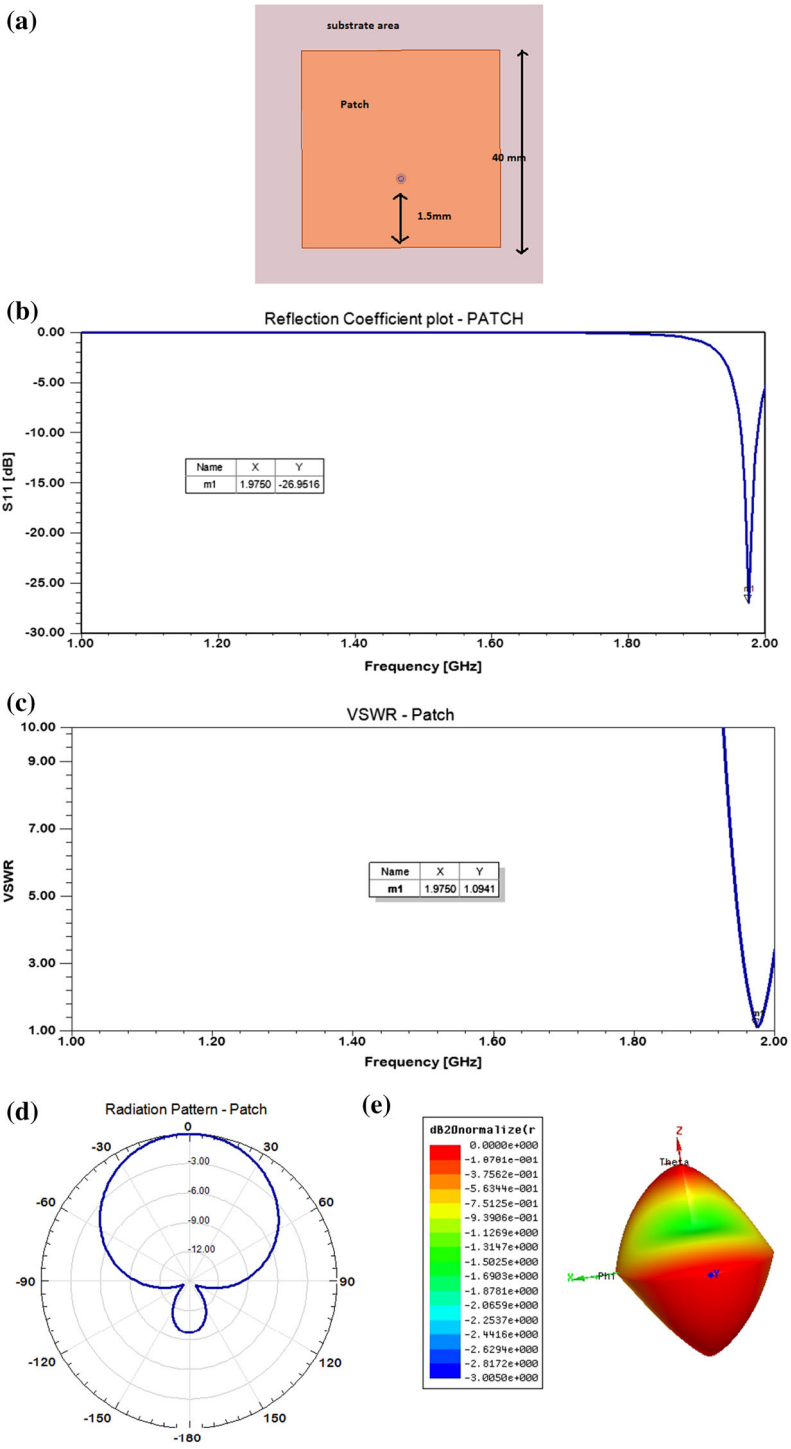
(a)
substrate area
Patch
40 mm
1.5mm
(b)
Reflection Coefficient plot - PATCH
S11 [dB]
Frequency [GHz]
Name X Y
m1 1.9750 -26.9516
(c)
VSWR - Patch
VSWR
Frequency [GHz]
Name X Y
m1 1.9750 1.0941
(d)
Radiation Pattern - Patch
(e)
dB20normalize(r
Theta

◀**Fig. 8** **a** Square patch geometry. **b** Reflection coefficient plot. **c** VSWR plot. **d** Radiation Pattern polar plot. **e** 3D radiation pattern

$$fr = \begin{cases} (0.15345 + 0.34\rho x)\dfrac{c}{h_e}(\xi^{-1}) & for\ n = 0 \\ 0.26\dfrac{c}{h_e}\delta^n & for\ n > 0 \end{cases}$$

$$x = \begin{cases} 0 & k = 0 \\ 1 & k > 1 \end{cases}$$

where $h_e = \frac{\sqrt{3S_e}}{2}$, $S_e = S + t(\varepsilon_r)^{-0.5}$ and $\delta =$ scale factor of the geometry, $\xi = \frac{1}{\delta}$ and $\rho = \xi - 0.230735$.

2.3 Simulation of SPK5 (5 Iteration SPK)

The geometry of the SPK monopole after five iterations is as shown in the Fig. 3. The height of the monopole is 90 mm and base of the initiator triangle is 102 mm. Five iterations state that it has five bands of operation as shown in the Fig. 4.

The reflection coefficient of the simulated SPK5 geometry is as shown in the Fig. 5a and the corresponding VSWR is presented in Fig. 5b. A study of reflection coefficient characteristics from Fig. 5a, reveals various resonant frequencies at which the computed value takes minima. It can be inferred from the reflection coefficient characteristics that at five different frequencies (i.e., 2.54, 3.56, 5.17, 6.49, 8.84 GHz) there is considerable S11 magnitude of less than −10 dB. Other dips which are above the reference level are ignored.

To understand the multifrequency characteristics of an antenna a study of the reflection coefficient curves alone is not sufficient it may show a very low reflection coefficient in some modes with exhibiting the desired radiation pattern. To support the same, radiation pattern reports are generated at the resonant frequencies as shown in the Fig. 6a through Fig. 6h. Figure 6a–d represent the distribution of the field for all θ and Ø = 0° and Fig. 6e–h represent the distribution of the field for all θ and Ø = 90°. Similarly VSWR values at the resonating frequencies are considerably good in analogous to reflection coefficient curve.

3 Miniaturisation Characteristics of SPK Bowtie

As discussed earlier in the introduction part, the investigations for miniaturisation of the antenna with FG are carried on SPK Bowtie geometries on microstrip patch antenna. The study is subdivided into four cases. The experiment is carried with a square patch as initiator which is referred as case 1. In case 2 a Bowtie is carved on the Square patch of case 1. A SPK geometry is patterned on Bowtie of case 2 to frame the case 3 experiment. A next iteration is observed on case 3 geometry to form the case 4 geometry. This is depicted in the following Fig. 7. All the geometries are designed using effective CAD tool integrated in HFSS and then simulated and solved using the effective FEM engine. Throughout all the cases the ARLON 320C substrate is considered with copper coating on both sides of the substrate. The patch is patterned on top side of the antenna and bottom side forms the ground plane. The height of the substrate is 1.6 mm.

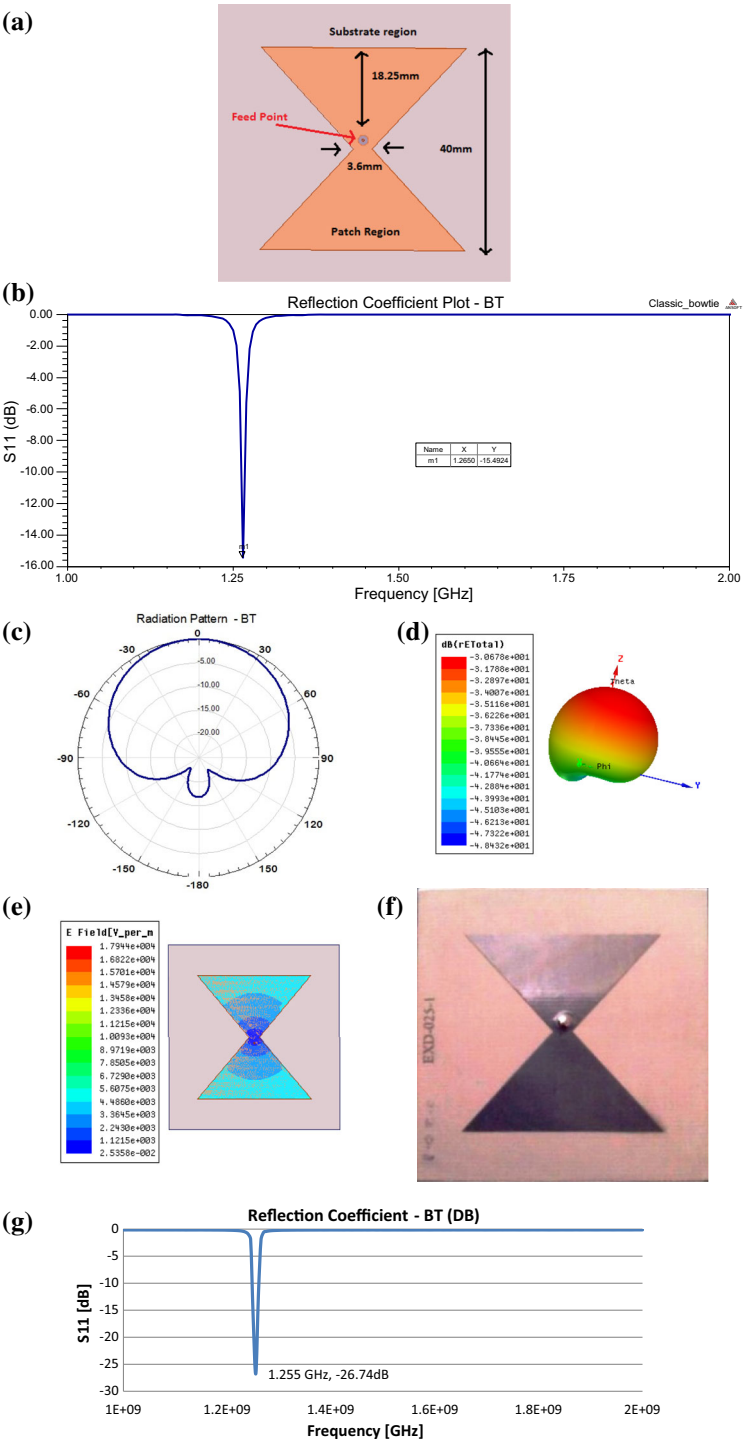
(a)
Substrate region
18.25mm
Feed Point
40mm
3.6mm
Patch Region
(b)
Reflection Coefficient Plot - BT
Classic_bowtie
S11 (dB)
Frequency [GHz]
Name X Y
m1 1.2650 -15.4924
(c)
Radiation Pattern - BT
(d)
dB(rETotal)
Theta
Ph1
(e)
E Field[V_per_m
(f)
EXD-025-1
(g)
Reflection Coefficient - BT (DB)
S11 [dB]
1.255 GHz, -26.74dB
Frequency [GHz]

◀**Fig. 9** **a** Geometry of Bowtie. **b** Reflection coefficient curve of BT. **c** Polar radiation plot. **d** 3D radiation pattern. **e** E-field distribution representation on BT. **f** Fabricated BT prototype. **g** Measured reflection coefficient of the fabricated prototype

All the antennas and the reports pertaining to the characteristics are presented as follows. For every case, frequency versus reflection coefficient plot, frequency versus VSWR plot, E-field distribution, Radiation Characteristics in 2D polar plot, 3D format and Frequency versus Directivity plots are taken using terminal solution reports menu in HFSS. Every report has a scope for investigation of various characteristics of the antenna with its own significance. The resonating frequency is identified from the reflection coefficient graphs for those dip values which have S11 less than −10 dB. The identified resonating frequency is confirmed if the VSWR value at that frequency from the VSWR report is below two. The radiation characteristics of the proposed geometry are studied from the 2D polar and 3D radiation plots.

These plots are taken at the resonating frequency or frequencies identified from the RC and VSWR plots. As all the antennas belong to a class of patch antennas the polar plot of the radiation pattern should have single major lobe on the upper zone and minor lobe or no lobe on the lower region. This shall be treated as the template pattern diagram for the patch antenna in any form. Hence it should be understood that the identified dip frequency from S11 plot has to be considered as resonating frequency only if it posses the template radiation pattern of the patch [15–19]. The Frequency versus Directivity plot will be useful to study the directivity characteristics of the antenna over every sweep frequency. The resonating frequency should report good directivity with a value greater than one which is the directivity of isotropic antenna. The plot is drawn between frequency and peak directivity in some direction. The works mentioned in [20–22] motivated us to develop this antenna design study.

3.1 CASE 1: Square Patch

The designed square patch antenna geometrical dimensions are as shown in the Fig. 8a. The side dimension is 40 mm. This simulated square patch is used as an initiator for the next generations of the experiment. The feed point is optimized and placed at 1.5 mm along positive Y axis. The Reflection Coefficient (RC) curve over a range of 1–2 GHz and the corresponding VSWR plot are as shown in the Fig. 8b, c. From the RC plot it can be read that the antenna shows a minimum dip at 1.975 GHz. This dip frequency is supported by the minimum value under 2 in the VSWR characteristics. With these 2 reports the resonating frequencies of the square patch antenna can be concluded as 1.975 GHz.

The radiation characteristics of the patch antenna are as shown in the Fig. 8d and the corresponding 3D plot is Fig. 8e. These two reports are taken at the resonating frequency investigated from the reflection coefficient and the VSWR plots.

3.2 CASE 2: Classic Bowtie

A bowtie antenna is formed by attaching two triangular patches connected at the short edges. The geometry of the simulated classic bowtie is as shown in the Fig. 9a. This geometry is derived from the square patch which is discussed on the case 1 section. The channel describes the current through put along these two triangular arms. In this proposed geometry, the width of the adjoining channel is 3.6 mm. The feed point is located at

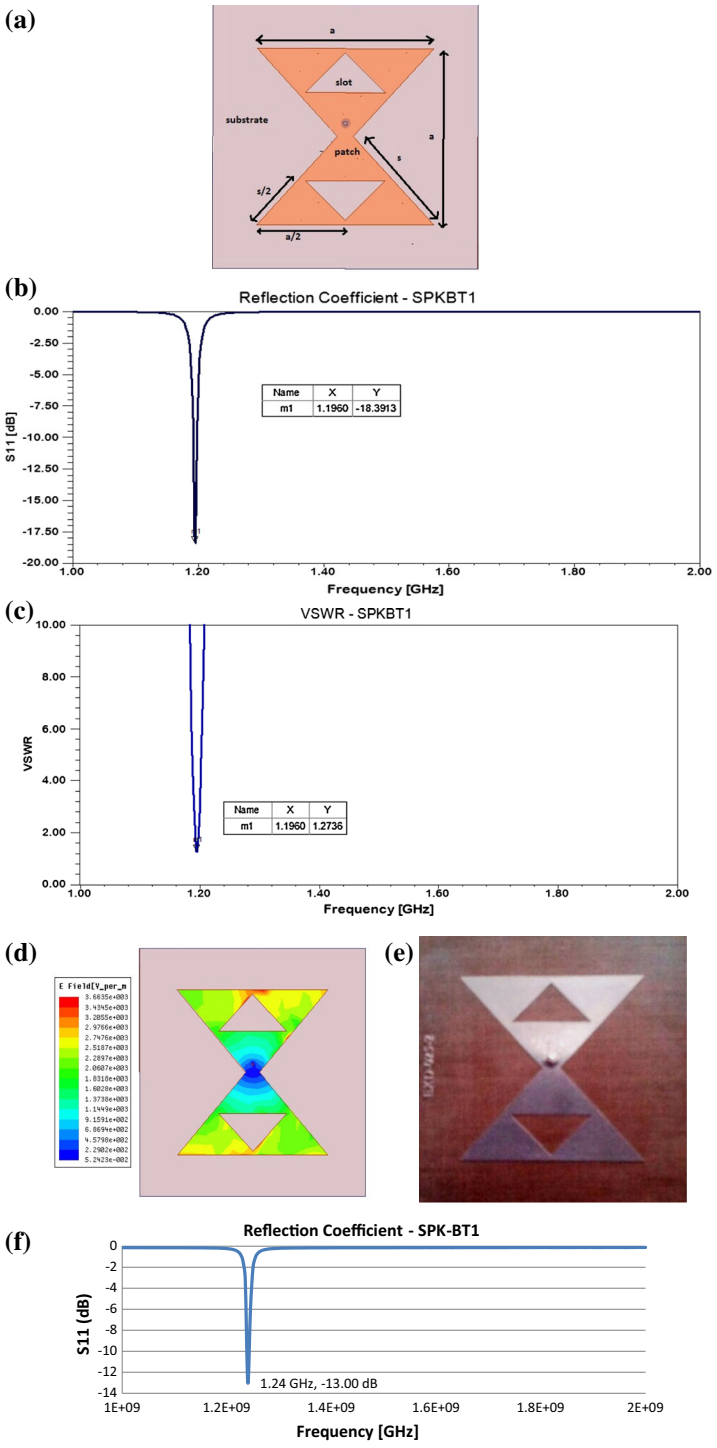
(a)
a
slot
substrate
patch
a
s
s/2
a/2
(b)
Reflection Coefficient - SPKBT1
S11 [dB]
Frequency [GHz]
Name X Y
m1 1.1960 -18.3913
(c)
VSWR - SPKBT1
VSWR
Frequency [GHz]
Name X Y
m1 1.1960 1.2736
(d)
(e)
(f)
Reflection Coefficient - SPK-BT1
S11 (dB)
1.24 GHz, -13.00 dB
Frequency [GHz]

◀**Fig. 10** **a** SPK Bowtie-1 geometry. **b** Simulated reflection coefficient plot. **c** VSWR plot. **d** E-field distribution. **e** Fabricated prototype of SPKBT-1. **f** Measured reflection coefficient of the prototype

1.75 mm from the center towards the +ve Y-axis. The reflection coefficient report obtained for the simulated geometry is presented in the Fig. 9b. The resonating frequency is identified as 1.2650 GHz from the RC plot. The corresponding radiation pattern polar plot is drawn at this operating frequency and is as shown in the Fig. 9c and the corresponding 3D radiation pattern is Fig. 9d. The fabricated prototype photograph is presented in the Fig. 9f. The geometry is etched using chemical wash on the arlon 320c purchased from a local vendor. Agilent 8719ES model network analyzer is used for reflection coefficient and VSWR measurements. Initially the cable losses are nullified in open-cal conditions by calibrating it to 0 dB. The start and stop frequencies are 1 and 2 GHz respectively. The curve displayed on the screen is converted into tabular form file with.csv extension. Then this data is imported into excel and finally a plot is drawn as shown in the Fig. 9g.

3.3 Case 3: SPK Bowtie-1 (SPKBT-1)

Figure 10a shows the proposed geometry of the SPKBT-1. This is obtained by taking the triangular geometry on the both the arms of the Bowtie antenna to 1st iteration of SPK. The terminals of the inner triangle are the midpoints of the outer triangle to depict a scaling factor of 2. The resonant frequency from the simulated reflection coefficient curve (Fig. 10b) of the SPKBT-1 is identified as 1.196 GHz. This is well supported by the VSWR plot as shown in the Fig. 10c. The fundamental mode of the operation can be studied from the E-field distribution plot of Fig. 10d. The fabricated prototype of the proposed geometry is as shown in the Fig. 10e. The measured S11 over sweep frequencies of 1–2 GHz are saved to excel file format from the vector Network Analyzer directly. Figure 10g shows the measured S11 (dB) plot. The resonant frequency from this plot is 1.24 GHz. This less than the classic BT antenna investigated in the earlier case.

3.4 CASE 4: SPK Bowtie-2 (SPKBT-2)

The geometry of the SPKBT-2 obtained by taking an iteration further over the previous geometry mentioned in the case 3 is as shown in the Fig. 11a. The simulated reflection coefficient curve of the designed SPKBT-2 as shown in Fig. 11b reads the resonating frequency as 1.14 GHz with an S11 value well below the −10 dB reference level. The corresponding radiation patterns in 2D and 3D at resonating frequency obtained from the RC plot are shown in the Fig. 11c, d. The fundamental mode operation and the corresponding field distribution can be observed from the Fig. 11e.

The fabricated prototype of the SPKBT-2 is as shown in the Fig. 11f. Figure 11g is the screen shot of the Vector Network Analyzer screen while the S11 of the prototype is displayed. This data is exported to MS Excel and then plotted to identify the resonant frequency which is 1.17 GHz according to Fig. 11h. The measured resonant frequency is less than the earlier SPKBT-1 geometry keeping the similar trend from square patch to SPKBT-2.

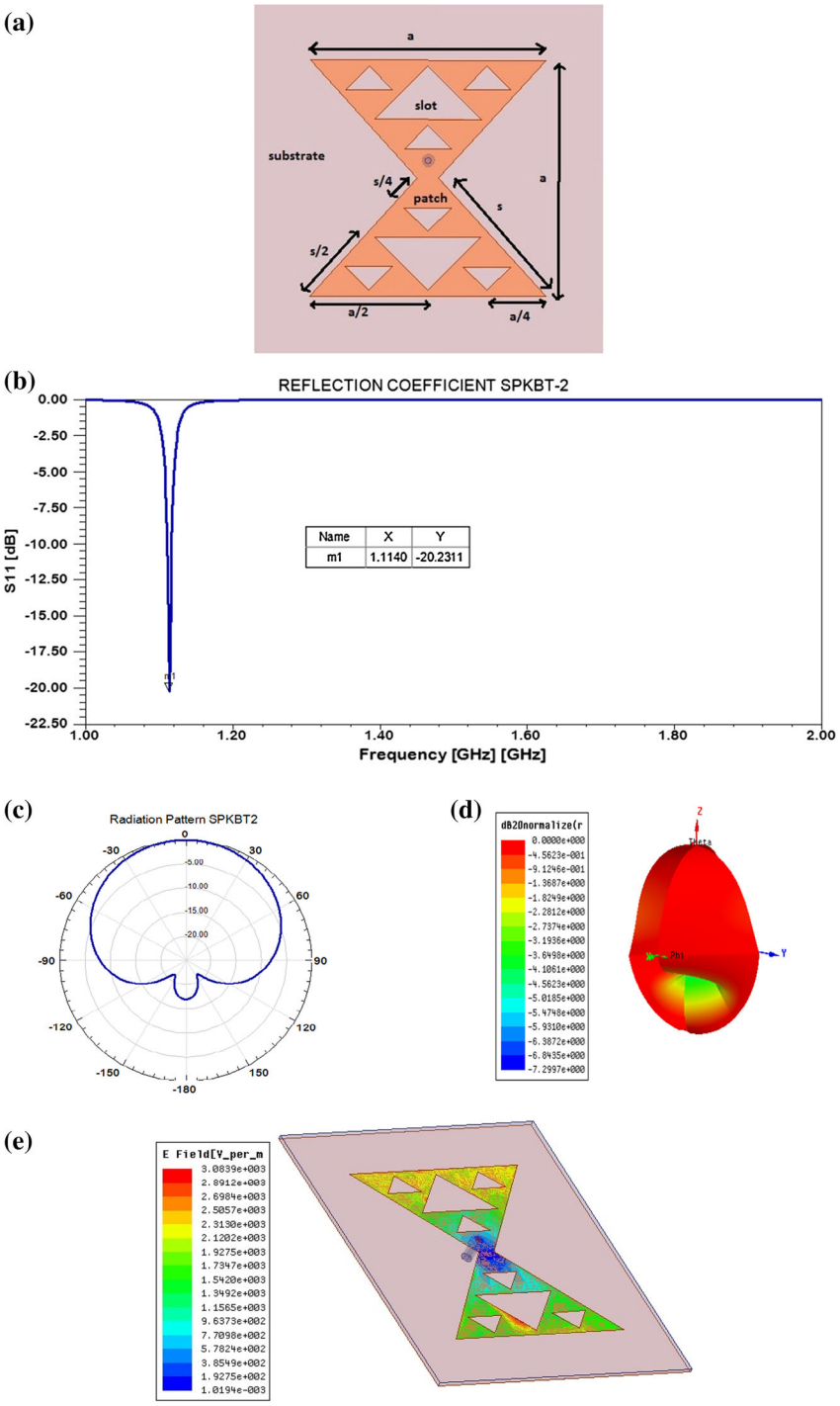
(a)
a
slot
substrate
s/4
patch
a
s
s/2
a/2
a/4
(b)
REFLECTION COEFFICIENT SPKBT-2
S11 [dB]
0.00
-2.50
-5.00
-7.50
-10.00
-12.50
-15.00
-17.50
-20.00
-22.50
Name X Y
m1 1.1140 -20.2311
1.00
1.20
1.40
1.60
1.80
2.00
Frequency [GHz] [GHz]
(c)
Radiation Pattern SPKBT2
0
30
60
90
120
150
-180
-150
-120
-90
-60
-30
-5.00
-10.00
-15.00
-20.00
(d)
dB20normalize(r
0.0000e+000
-4.5623e-001
-9.1246e-001
-1.3687e+000
-1.8249e+000
-2.2812e+000
-2.7374e+000
-3.1936e+000
-3.6498e+000
-4.1061e+000
-4.5623e+000
-5.0185e+000
-5.4748e+000
-5.9310e+000
-6.3872e+000
-6.8435e+000
-7.2997e+000
Z
Theta
Phi
Y
(e)
E Field[V_per_m
3.0839e+003
2.8912e+003
2.6984e+003
2.5057e+003
2.3130e+003
2.1202e+003
1.9275e+003
1.7347e+003
1.5420e+003
1.3492e+003
1.1565e+003
9.6373e+002
7.7098e+002
5.7824e+002
3.8549e+002
1.9275e+002
1.0194e-003

◀**Fig. 11** **a** Geometry of the SPKBT-2. **b** Simulated reflection coefficient of the SPKBT-2 geometry. **c** Radiation pattern. **d** 3D Radiation pattern. **e** E-field distribution. **f** Fabricated prototype of SPKBT-2. **g** Network analyzer. **h** Measured S11 of the prototype

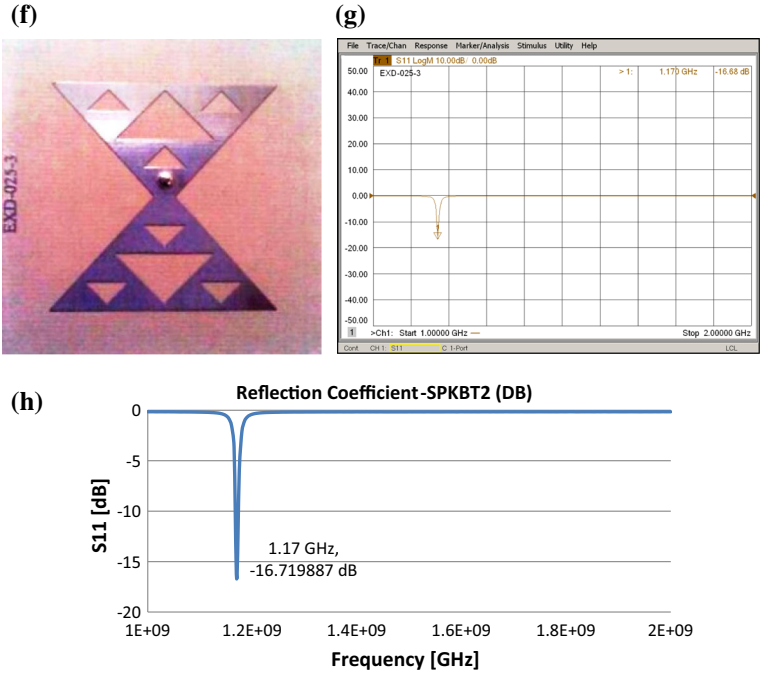

Fig. 11 continued

Table 1 Tabulated measured and simulated resonant frequencies of various geometries

Geometry	Resonant frequency (GHz) (simulation)	Resonant frequency (GHz) (measured)
Square patch	1.975	–
Bowtie	1.265	1.255
SPKBT-1	1.196	1.24
SPKBT-2	1.114	1.17

3.5 Concept of Miniaturization in SPK Bowtie

The resonant frequencies obtained from the above four cases are tabulated in Table 1. From the square patch to SPKBT-2 the effective area is diminishing and the corresponding resonant frequencies are also observing a decrease similarly. It is observe that the height of the antenna is made constant with diminishing operating frequency. This is made possible by carefully patterning the SPK geometry on the surface of the antenna. This shift in the operating frequency can also be controlled by the scaling factor of the SPK.

4 Conclusion

The multiband characteristics of Sierpinski Fractal antenna are well explored in terms of several parameters and reports like reflection coefficient, VSWR and radiation pattern plots. Under miniaturisation category a Sierpinski Bowtie is considered and various characteristics are analyzed. Starting from patch to Bowtie and further at each iteration the resonating frequency decreases considerably with diminishing surface area. This clearly manifests miniaturization characteristics with increased directivity. Complexity is always involved with the fabrication of these typical antennas, which can be minimized by proposing modified fractal shapes. A study of the trend of the bandwidth with change in frequency would have a good scope of future work.

References

1. Anguera, J., Puente, C., Borja, C., & Soler, J. (2005). Fractal shaped antennas: A review. Encyclopedia of RF and Microwave Engineering.
2. Żotkiewicz, M., & Pióro, M. (2013). Exact approach to reliability of wireless mesh networks with directional antennas. *Telecommunication Systems, 56*, 1–11.
3. Mandal, D., Ghoshal, S. P., & Bhattacharjee, A. K. (2013). Optimized radii and excitations with concentric circular antenna array for maximum sidelobe level reduction using wavelet mutation based particle swarm optimization techniques. *Telecommunication Systems, 52*(4), 2015–2025.
4. Carle, G., & Zitterbart, M. (2002). *Proceedings of the 7th IFIP/IEEE international workshop on protocols for high speed networks*.
5. Freeman, W. H., & Jabbar, W. H. (2011). New elements concentrated planar fractal antenna arrays for celestial surveillance and wireless communications. *ETRI Journal, 33*(6), 849–856.
6. Lizzi, L., Azaro, R., Oliveri, G., & Massa, A. (2012). Multiband fractal antenna for wireless communication systems for emergency management. *Journal of Electromagnetic Waves and Applications, 26*(1), 1–11.
7. Werner, D. H., & Werner, P. L. (1996). Frequency-independent features of self-similar fractal antennas. *Radio Science, 31*(6), 1331–1343.
8. Mushiake, Y. (1992). Self-complementary antennas. *Antennas and Propagation Magazine, IEEE, 34*(6), 23–29.
9. Chowdary, P. S. R., Prasad, A. M., Rao, P. M., & Anguera, J. (2013). Simulation of radiation characteristics of Sierpinski fractal geometry for multiband applications. *International Journal of Information and Electronics Engineering, 3*(6), 618–621.
10. Vinoy, K. J., Jose, K. A., & Varadan, V. K. (2004). Generalized design of multi-resonant dipole antennas using Koch curves. *Applied Computational Electromagnetics Society Journal, 19*(1), 22–31.
11. Puente-Baliarda, C., Romeu, J., Pous, R., & Cardama, A. (1998). On the behavior of the Sierpinski multiband fractal antenna. *IEEE Transactions on Antennas and Propagation, 46*(4), 517–524.
12. Anagnostou, D., Chryssomallis, M. T., Lyke, J. C., & Christodoulou, C. G. (2003). Improved multiband performance with self-similar fractal antennas. *IEEE Topical Conference on Wireless Communication Technology, 271*, 272.
13. Na, Y., & Xiao-wei, S. (2005). Analysis of the multiband behavior on Sierpinski carpet fractal antennas. *Asia-Pacific Microwave Conference Proceedings, 4*, 10–14.
14. Mishra, R. K., Ghatak, R., & Poddar, D. R. (2008). Design formula for Sierpinski gasket pre-fractal planar-monopole antennas [Antenna Designer's Notebook]. *IEEE Antennas and Propagation Magazine, 50*(3), 104, 107.
15. Anguera, J., Puente, C., Borja, C., Montero, R., & Soler, J. (2001). Small and high directivity bowtie patch antenna based on the Sierpinski Fractal. *Microwave and Optical Technology Letters, 31*(3), 239–241.
16. Anguera, J., Montesinos, G., Puente, C., Borja, C., & Soler, J. (2003). An under-sampled high directivity microstrip patch array with a reduced number of radiating elements inspired on the Sierpinski fractal. *Microwave and Optical Technology Letters, 37*(2), 100–103.
17. Anguera, J., Martínez, E., Puente, C., Borja, C., & Soler, J. (2006). Broad-band triple-frequency microstrip patch radiator combining a dual-band modified Sierpinski fractal and a monoband antenna. *IEEE Transactions on Antennas and Propagation, 54*(11), 3367–3373.

18. Anguera, J., Puente, C., Borja, C., & Soler, J. (2007). Dual frequency broadband stacked microstrip antenna using a reactive loading and a fractal-shaped radiating edge. *IEEE Antennas and Wireless Propagation Letters, 6*, 309–312.
19. Anguera, J., Martínez, E., Puente, C., Borja, C., & Soler, J. (2004). Broad band dual-frequency microstrip patch antenna with modified Sierpinski fractal geometry. *IEEE Transactions on Antennas and Propagation, 52*(1), 66–73.
20. Kamakshi, K., Ansari, J. A., Singh, A., & Aneesh, M. (2014). Analysis of L-probe proximity fed annular ring patch antenna for wireless applications. *Wireless Personal Communications, 77*(2), 1449–1464.
21. Bilgiç, M. M., & Yeğin, K. (2014). Diversity antenna design for wireless alarm networks. *Wireless Personal Communications, 78*(1), 729–740.
22. Ansari, J. A., Kumari, K., Singh, A., & Mishra, A. (2013). Ultra wideband co-planer microstrip patch antenna for wireless applications. *Wireless Personal Communications, 69*(4), 1365–1378.

P. Satish Rama Chowdary received M.Tech in Radar and Microwave Engg from Andhra University in the year 2009. He is currently pursuing Ph.D. in Department of Electronics & Communication Engg, JNTUK, Kakinada, India. He is working in the Department of ECE, Raghu Institute of Technology, Visakhapatnam, India. His area of interest includes Computational Electromagnetics and Antennas. He is a Life Member of Institute of Electronics and Telecommunication Engineers (IETE) and Instrument Society of India (ISI).

A. Mallikarjuna Prasad did his B.Tech in ECE from Nagarjuna University, during 1984–1988. He did his M.Tech in Electronics & Instrumentation from Andhra University in 1992 and completed his Ph.D. in 2009 from JNTU in the field of Antennas. He has joined JNT University service as Associate Professor of ECE in June 2003. He got promoted as Professor in ECE during Nov 2011. He has 20 publications in various International and National Journals and conferences. His areas of interest includes Antennas and Bio-Medical Instrumentation. He is a Life Member of Society of EMC Engineers (India), Indian Society for Technical Education (ISTE), Institute of Electronics and Telecommunication Engineers (IETE), and Instrument Society of India (ISI). He won best teacher award by student evaluation of 2008 batch.

P. Mallikarjuna Rao received B.E., M.E. and Ph.D. degrees from Andhra University, Visakhapatnam. He is a recipient of Best Ph.D. Award during 1999. He joined as Assistant Professor in the Department of ECE, Andhra University in 1990 and became Associate Professor in 1994 and Professor in 2002. He is Chairman, Board of Studies, ECE, Andhra University. Prior to this he served as Assistant Professor in SRKR College of Engineering, Bheemavaram during 1985–1990. His areas of interest include Antennas and Bio Medical Signal Processing. He has 19 International Journal publications and 31 International and National Conferences papers.

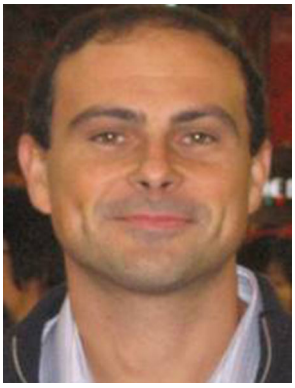

Jaume Anguera was born in Vinaròs, Spain, in 1972. He received the Technical Ingeniero degree in electronic systems and Ingeniero degree in electronic engineering, both from the RamonLlull University (URL), Barcelona, Spain, in 1994 and 1997, respectively, and the Ingeniero and Ph.D. degrees in telecommunication engineering from the Polytechnic University of Catalonia (UPC), Barcelona, Spain, in 1998 and 2003, respectively. He published more than 150 papers in National, International Journals and Conferences. He has chaired for many International and National conferences organized by URSI, IEEE etc. He has 70 granted patents, 50 patent applications and 31 patent families. He is reviewer of many international journals like IEEE, IEE Electronics Letters, PIERS, ETRI etc. He is the author of books titled "Antenna Theory" and "Antennas: An interactive approach". Since 2005, he is leading a research in antenna for handset and wireless devices in the frame of University-Industry collaboration with Fractus, S.A. and University Ramon Llull. He has been participating in 10 national projects, as principal investigator in some of them.